The First Extragalactic Exoplanets — What We Gain From High Cadence Observations of the Small Magellanic Cloud?

Radosław Poleski*and Przemek Mróz†

November 2018

Abstract

We propose to increase LSST cadence for the Small Magellanic Cloud which will enable finding dozens of microlensing events annually and potentially, a few planetary events over the course of the survey. These would be the first extragalactic exoplanets ever discovered and will give us a unique constraint on the planet formation and evolution in different environments. We discuss what changes in the LSST observing strategy are required. Presented analysis takes into account an extensive photometric follow-up program.

1 White Paper Information

Please contact Radek Poleski, `radek.poleski@gmail.com`, with any questions about this white paper.

1. **Science Category:** Exploring the Changing Sky
2. **Survey Type Category:** mini survey
3. **Observing Strategy Category:** an integrated program with science that hinges on the combination of pointing and detailed observing strategy (e.g., search for variable stars in the LMC/SMC).

*Department of Astronomy, Ohio State University, 140 W. 18th Ave., Columbus, OH 43210, USA
†Warsaw University Observatory, Al. Ujazdowskie 4, 00-478 Warszawa, Poland

2 Scientific Motivation

Deep understanding of planet formation and evolution requires studying planets in a wide range of environments. Currently known exoplanets are situated in the Milky Way and most of them are found close to the Sun because of higher sensitivity of transit and radial velocity techniques for brighter (hence nearby) host stars. Discovering extragalactic exoplanets is even more challenging than finding the Milky Way planets because of larger distances. We propose high cadence observations of the Small Magellanic Cloud (SMC) by LSST, and show that these observations will allow finding extragalactic exoplanets using gravitational microlensing technique.

Microlensing is sensitive to the lens mass, not light, hence, it allows one to find very faint objects. Previous microlensing discoveries include: a Neptune-mass free floating planet (Mróz et al. 2018), an Earth-mass planet around a brown dwarf (Shvartzvald et al. 2017), and a binary lens with a stellar remnant (Shvartzvald et al. 2015). For the SMC events, in most cases even the light from the planet host will not be detectable. Microlensing searches of exoplanets in M31 have not yet found planets, mainly due too a small number of events (Ingrosso et al. 2009; Calchi Novati et al. 2014; Lee et al. 2015). The other possibility of finding extragalactic exoplanets with LSST — the transit method applied to the Large Magellanic Cloud (LMC) — requires a dedicated Deep Drilling field (which is a larger effort than proposed here) and candidate transits will be very difficult to confirm using even the next generation 30-m telescopes (Lund et al. 2015; Jacklin et al. 2015). In Mróz & Poleski (2018) we proposed to observe the SMC with higher cadence, so that microlensing events can be found early and detection of planetary signatures in these events could be done using LSST data (if cadence is high enough) or using photometric follow-up observations from smaller telescopes. Microlensing events observed toward the SMC are almost exclusively of self-lensing type, i.e., both the lens and the source are in the SMC (Sahu & Sahu 1998; Wyrzykowski et al. 2011). As the SMC is stretched and elongated along the line-of-sight, the microlensing event rate is boosted.

There are thousands of microlensing events discovered so far toward the Galactic bulge. Among these events, about 70 planetary events have already been published and more are being analyzed. The planetary companion to the microlensing host star shows its presence via a short-lasting anomaly (Mao & Paczyński 1991; Gould & Loeb 1992) on top of a point-source point-lens event (Paczyński 1986). The length of the anomaly is on the order of the Einstein timescale of the host event multiplied by a square root of the mass ratio. Galactic bulge microlensing events have typical Einstein timescales of ≈ 20 days, hence, giant planets produce signals that last on the order of 1 day. The current Galactic bulge microlensing surveys (mainly KMT, OGLE-IV, and MOA-II, but also Wise and UKIRT) have cadence of up to 15-20 minutes which allows robust detection of gas- and ice-giant exoplanets using survey data only (e.g., Yee et al. 2012; Poleski et al. 2014; Shvartzvald et al. 2016). The alternative approach is to follow-up events found by surveys with a network of follow-up telescopes which can have small field-of-view cameras and, in many cases, smaller apertures. Follow-up observations are particularly useful for high-magnification events (peak magnifi-

cation $\gtrsim 100$), which both have higher planet detection efficiency and can be recognized in advance (Griest & Safizadeh 1998; Gould et al. 2010). The median Einstein timescale of SMC events is ≈ 3 times longer than that of Galactic bulge events which leads to longer timescales of planetary anomalies. One-hour cadence in the SMC should be enough to efficiently detect and characterize gas-giant planets.

The two planet parameters that are readily measured for microlensing planets are the mass ratio q and the star-planet projected separation s, which is expressed in units of the Einstein ring radius ($\theta_{\rm E}$). The Einstein ring radius is a characteristic angular scale of the microlensing events. Median value of $\theta_{\rm E}$ projected to the SMC distance corresponds to 3 AU. The detection efficiency is highest for planets with $0.7 < s < 1.6$, which translates to a range from 2 AU to 5 AU. Median mass of the lens for the SMC events is 0.35 $M_\odot$ and the snow line (which is the location in the proto-planetary disk where the water ice may condense and where gas giant planets are believed to form) lies at $\approx 2.7\,(M/M_\odot)$ AU. Planets probed in the proposed experiment lie outside the snow lines of their hosts.

In Figures 1 and 2, we present the light curves of example microlensing events. First event is not detected in `baseline_2018a` OpSim run (Fig. 1, *upper panel*). However, the event is clearly detected with enhanced LSST coverage as proposed here (Fig. 2, *lower panel*). The event detection allows follow-up observations to be conducted (pink symbols for Chilean and gray for non-Chilean). The planetary anomaly on fading branch is clearly detected with $\Delta\chi^2 = 6200$ when compared to the point-source point-lens model. All datasets are scaled to a single magnitude system (r in this case) using source and blending fluxes. The Einstein timescale is 145 d, $s = 0.96$, and $q = 1.2 \times 10^{-4}$. The second event (Fig. 2) is a high magnification event (maximum magnification ≈ 80) and the planet with $s = 1.04$, $q = 7.9 \times 10^{-4}$ is detected with $\Delta\chi^2 = 2900$ in proposed strategy. The event timescale is 89 d and it is detected at JD = 2463037.

The LSST telescope and camera have unique capability to study microlensing events toward the SMC. The photometry from the on-going microlensing surveys is not deep enough to detect statistically significant number of SMC events. The LSST field of view is large enough to cover large part of region of interest in just two pointings.

It is possible that planet frequency in the SMC is lower than in the Solar neighborhood. The correlation between stellar metallicity and planet frequency is well known (Fischer & Valenti 2005; Wang & Fischer 2015), but without performing proposed experiment we cannot be sure if it applies to smaller-mass hosts and wider orbit planets, which are probed by microlensing. Below we present expected yield that assumes a fiducial planet frequency function and request the experiment with yield of a few planets so that, scientifically interesting upper limits on the planet frequency can be derived even if no planets are detected.

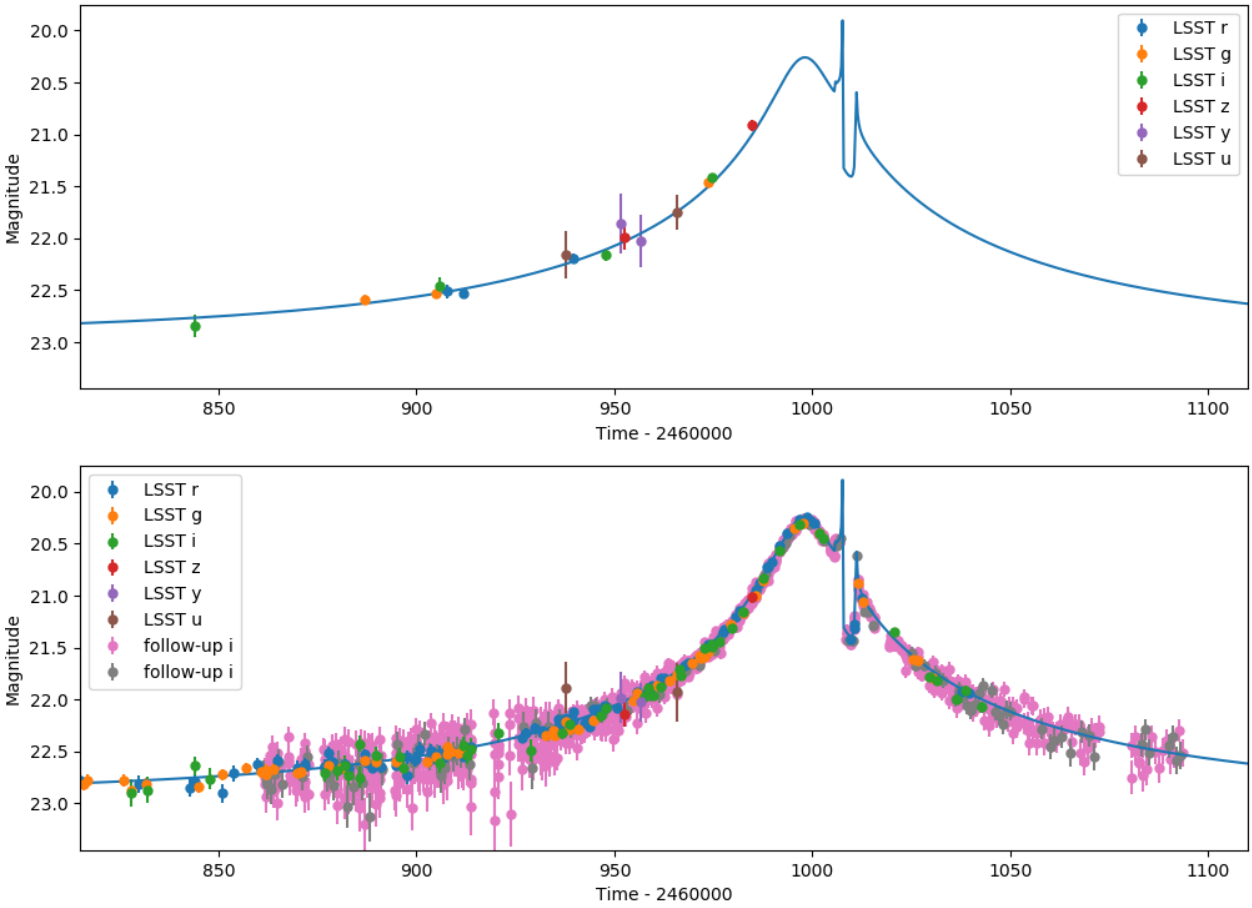

Figure 1: Example light curves of a planetary microlensing event. *Upper panel* shows light curve in `baseline_2018a` OpSim run. *Lower panel* shows light curve with enhanced coverage as proposed here.

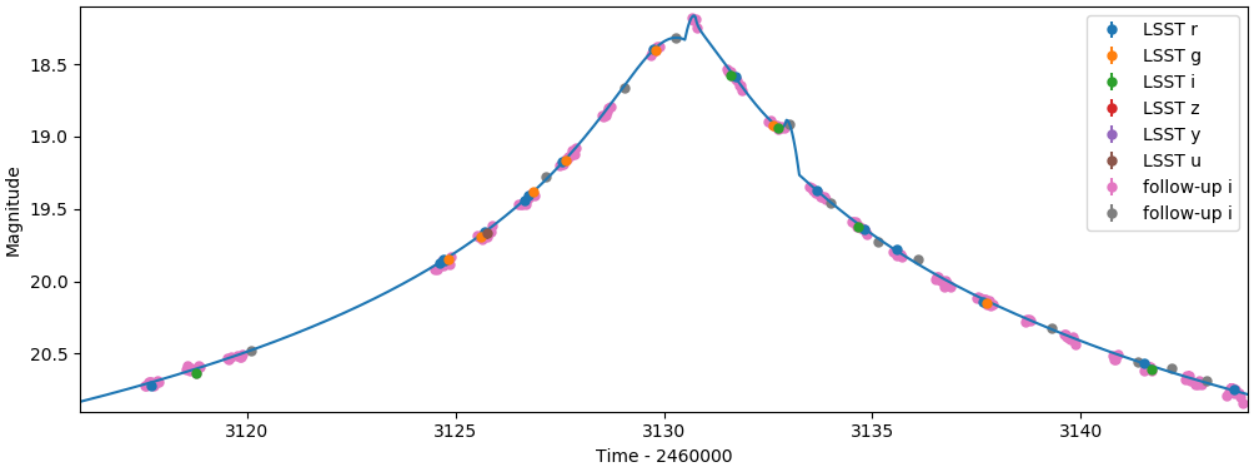

Figure 2: Example light curve of a high-magnification planetary microlensing event.

3 Technical Description

3.1 High-level description

Here we present technical description of a program where LSST sampling is sufficient to discover microlensing events in the SMC, while most of planet sensitivity comes from the follow-up observations. If most of the planet sensitivity comes from the LSST observations, then the cadence would need to be improved to 1 hour.

We propose for on the order of 2000 visits to be taken in each of two fields in the center of the SMC. The sampling should be uniform in time and r, g, and i filters give the highest yield.

3.2 Footprint – pointings, regions and/or constraints

The large field of view of LSST allows covering almost the entire sky-region of interest in two pointings centered at (R.A., Dec.) of $(17.58°, -72.40°)$ and $(9.62°, -73.82°)$. These fields were selected with constrained that their separation is similar to separations of fields in `baseline_2018a` OpSim run. If only a single pointing is chosen, then it should be placed at $(14.50°, -73.00°)$.

3.3 Image quality

Due to high crowding of the field, we request observations with seeing < 2 arcsec.

3.4 Individual image depth and/or sky brightness

We request r and g band image depths of $\gtrsim 23.5$ mag and i band depth of $\gtrsim 23.0$ mag. The depths may be relaxed at the beginning and end of the SMC observing season in order to extend the time coverage each year, during which the data are collected.

The SMC is located far from Ecliptic, hence, it can be observed independently of the Moon phase.

3.5 Co-added image depth and/or total number of visits

The high detection efficiency of microlensing events requires a uniform sampling and a cadence on the order of 1 day. This translates to on the order of 2000 visits after accounting for visibility and weather constraints.

There is no direct constraint on the co-added image depth.

3.6 Number of visits within a night

The optimal strategy is to take one or two visits per night. If there are multiple visits during one night, then they should be separated by at least 1 hour.

3.7 Distribution of visits over time

The detection of microlensing events is best done with a uniform sampling. We request higher cadence at the beginning of the survey (until at least > 15 epochs are collected in r, g, and i bands), because microlensing events can be found only after establishing which stars are constant. In order to achieve a uniform cadence, it may be necessary to observe the field at airmass as large as 2.0.

3.8 Filter choice

The number of observable sources is the largest in the r band. The slightly smaller number of visible sources is in the g band, and the third best filter is i. Hence, we request the relative number of epochs to be $4 : 2 : 1$ in r, g, and i bands, respectively. Having multi-band observations is important in order to characterize the properties of sources in microlensing events.

3.9 Exposure constraints

We request standard 2×15 s or 1×30 s visits. The total exposure time per visit is constrained by the desired depth of a single visit. Saturation of the brightest objects is not an issue, because there are almost no events with sources saturated in standard LSST visits and if an event becomes brighter than the saturation limit, then the follow-up resources will provide an adequate photometric coverage.

3.10 Other constraints

There are no other constraints.

3.11 Estimated time requirement

The exposure time (30 s) plus shutter open/close is 32 s. The slew time is going to be relatively short. The closest field that is observed with the standard Wide-Fast-Deep cadence in `baseline_2018a` is separated by 11°. More importantly, one of the Deep Drilling fields (namely R.A. = 23.29°, Dec. = −63.32°) is located only 13° away. Observations of this Deep Drilling field give many chances to slew to the SMC fields without too much overhead on slew and filter change. We estimate that typical slew and settle time will be 15 s for the first field and 5 s for the second field. We also estimate that a quarter of the visits will require filter change, which takes 120 s. The average total time of a visit in both fields is

thus 120 s/4 + 15 s + 32 s + 5 s + 32 s = 114 s. The total time requested for 2000 visits is only 63.33 h or 0.26% of the total time available (24236 h). If a single field is observed, then these numbers are 77 s, 42.78 h, and 0.18%, respectively.

Properties	Importance
Image quality	2
Sky brightness	3
Individual image depth	1
Co-added image depth	3
Number of exposures in a visit	3
Number of visits (in a night)	1
Total number of visits	1
Time between visits (in a night)	2
Time between visits (between nights)	1
Long-term gaps between visits	3
Other (please add other constraints as needed)	3

Table 1: **Constraint Rankings:** Summary of the relative importance of various survey strategy constraints. Please rank the importance of each of these considerations, from 1=very important, 2=somewhat important, 3=not important. If a given constraint depends on other parameters in the table, but these other parameters are not important in themselves, please only mark the final constraint as important. For example, individual image depth depends on image quality, sky brightness, and number of exposures in a visit; if your science depends on the individual image depth but not directly on the other parameters, individual image depth would be '1' and the other parameters could be marked as '3', giving us the most flexibility when determining the composition of a visit, for example.

3.12 Technical trades

1. What is the effect of a trade-off between your requested survey footprint (area) and requested co-added depth or number of visits?

We request observations of two fields. If only a single optimally-placed field is observed with the same cadence, then the Figure of Merit presented below decreases by 19%.

There is no direct constraint on the co-added depth.

2. If not requesting a specific timing of visits, what is the effect of a trade-off between the uniformity of observations and the frequency of observations in time? e.g. a 'rolling cadence' increases the frequency of visits during a short time period at the cost of fewer visits the rest of the time, making the overall sampling less uniform.

The uniform cadence is requested and is most advantageous for the proposed science program. The increase of visit frequency (at the cost of lower frequency at other times)

will only help if short-lasting caustic-crossing features are predicted, but in those cases the follow-up resources should be used, not LSST.

3. What is the effect of a trade-off on the exposure time and number of visits (e.g. increasing the individual image depth but decreasing the overall number of visits)?

A decrease in overall number of visits is not desirable, because it will delay the detection of the microlensing events. It will allow additional very faint events to be observed, but their value will be lower due to the limited depth of the follow-up observations.

4. What is the effect of a trade-off between uniformity in number of visits and co-added depth? Is there any benefit to real-time exposure time optimization to obtain nearly constant single-visit limiting depth?

Only two fields are proposed here and a uniform sampling in time is more important than uniform depth of each visit.

5. Are there any other potential trade-offs to consider when attempting to balance this proposal with others which may have similar but slightly different requests?

We expect that there will be other proposals that request observations of the SMC and LMC (see Sec. 7 in Marshall et al. 2017). Most of the other proposals will probably put stronger requests on observing a large area of the Clouds at the expense of lower cadence. Our proposal is most beneficial at the center of SMC. We expect variability studies in the SMC (including planetary transits) will be optimized towards the largest number of stars monitored, which is in accordance with the plan proposed here. Observations in u, z, and y bands may be requested in other proposals, but these bands have low value for the science program proposed here. If observations in u, z, and y bands are executed in addition to our program, then they will improve the source characterization to a small degree. If a wide area around the center of the SMC is proposed in other proposals than combining these observations with our program will lower the overheads.

4 Performance Evaluation

To evaluate performance of particular observing strategy in achieving our science goals, we propose **Figure of Merit** (FoM), which is a number of the SMC planets discovered. The number is evaluated assuming a fiducial planet frequency and taking into account the follow-up observations, as described below. We provide software that evaluates FoM based on OpSim simulation. This software is not part of MAF package. Evaluating FoM for a single OpSim simulation with accuracy of 5% takes about 6 h.

In our simulations of detection efficiency, we have included intensive photometric follow-up observations. The optimum follow-up would be a uniform and 24-hour coverage of every on-going microlensing event with a high photometric accuracy. The SMC lies close to the South celestial pole and there is a limited number of observatories with good astronomical climate that can observe the SMC. There is a number of telescopes located in Chile, but they

cover a narrow range of longitudes. Outside Chile, the only observatories with large aperture telescopes are Siding Spring Observatory (Australia) and South African Astronomical Observatory (South Africa). The number of clear nights and seeing are better for Chilean observatories. Taking all these aspects into account, we divide the follow-up observations into Chilean and non-Chilean. For Chilean observatories, we assume observations are taken when the SMC center is at the altitude $> 30^\circ$ and Sun is at the altitude $< -15^\circ$ as seen from Cerro Pachón. We select nights for which these conditions are fulfilled for at least 30 min and assume uniform cadence of 1 h. To simulate the impact of clouds, we remove epochs for which there is no LSST observations (in any field) 1 h prior or after considered follow-up epoch. There are in total ten optical telescopes in Chile that have aperture of 4 m or larger. We assume that the follow-up observations will be conducted using a $\approx$ 4-m telescope and the same exposure time as for LSST. The same photometric accuracy should be achievable using longer (and still reasonable) exposure times on a 2-m class telescopes. To account for airmass, seeing, and sky transparency on photometric accuracy, we use the accuracy of the closest LSST observation with additional correction of $\delta m_5 = -0.53$ mag added to 5σ depth of LSST (for this we use the i-band observations in a few fields close to the SMC), see Ivezić et al. (2018).

The potential follow-up telescopes outside Chile have smaller apertures and poorer weather conditions. We simulate these additional follow-up epochs assuming there is a single epoch per night and it is shifted by 12 h relative to observations in Chile. Additionally, we select half of the nights only. To estimate photometric accuracy of these data, we follow the same procedure as for Chilean follow-up observations. For each event, the follow-up observations are assumed to start 12 h after the event detection and end $3t_{\rm E}$ after the event peaks.

The above strategy leads to on average 1400 follow-up epochs for Chilean observatories over 10-month long season in `baseline_2018a` run. For non-Chilean observatories there are on average 120 follow-up epochs per season.

We simulate planetary systems assuming the planet frequency as derived from recent microlensing studies in Galactic bulge fields: Suzuki et al. (2016) and Udalski et al. (2018). The planet frequency is a function of microlensing parameters: mass ratio q and projected separation s. For the SMC events, the Einstein ring radius is smaller than for bulge events, but the lens is at larger distance, and these two effects approximately cancel out. As a result, the values of s in the SMC that are probed by microlensing are similar to the values in the Galactic bulge fields. We may expect that the planet frequency is lower in the SMC, but for calculating the FoM, we assume the same as in the Galactic bulge and request sampling that leads to at least a few planets are discovered under this assumption.

To evaluate the FoM, we multiply the number of microlensing events in the monitored sky-area over the survey time-span by the fraction of events that show planetary anomalies with significance $\Delta\chi^2 > 100$. This fraction depends on input from OpSim. To estimate the number of events, we multiply event rate in the sky-area considered (2.7×10^{-7} yr^{-1}), the total number of sources in the SMC (1.7×10^9), the fraction of sources that are in monitored area (0.67), the fraction of sources in brightness range detectable with LSST (0.098), and the survey time-span (10 yr). This results in 293 events. We simulated an observing strategy

that follows our request and estimated the fraction of events that show detectable planetary anomalies to be 0.0097. Hence, the expected planet yield is 2.84. In `baseline_2018a` anomalies are detected for only 0.0017 of events and expected planet yield is 0.50. The threshold value of our FoM (at which point proposed science would be unsuccessful) is 2.5 and the ideal goal is 4.0.

The software for evaluating FoM is available at:

`https://github.com/rpoleski/LSST_SMC`

5 Special Data Processing

Standard photometric data processing of LSST data will be enough. There are several implementations of algorithms that find the microlensing events in large datasets. Also the algorithms for scheduling observations of follow-up telescopes have been implemented. We will build a dedicated pipeline that incorporates solutions from previous observing campaigns.

6 References

Calchi Novati, S., Bozza, V., Bruni, I., et al. 2014, ApJ, 783, 86

Fischer, D. A. & Valenti, J. 2005, ApJ, 622, 1102

Gould, A., Dong, S., Gaudi, B. S., et al. 2010, ApJ, 720, 1073

Gould, A. & Loeb, A. 1992, ApJ, 396, 104

Griest, K. & Safizadeh, N. 1998, ApJ, 500, 37

Ingrosso, G., Novati, S. C., de Paolis, F., et al. 2009, MNRAS, 399, 219

Ivezić, Ž., Kahn, S. M., Tyson, J. A., et al. 2018, ArXiv e-prints [`arXiv:0805.2366v5`]

Jacklin, S., Lund, M. B., Pepper, J., & Stassun, K. G. 2015, AJ, 150, 34

Lee, C.-H., Riffeser, A., Seitz, S., Bender, R., & Koppenhoefer, J. 2015, ApJ, 806, 161

Lund, M. B., Pepper, J., & Stassun, K. G. 2015, AJ, 149, 16

Mao, S. & Paczyński, B. 1991, ApJ, 374, L37

Marshall, P., Anguita, T., Bianco, F. B., et al. 2017, ArXiv e-prints [`arXiv:1708.04058`]

Mróz, P. & Poleski, R. 2018, AJ, 155, 154

Mróz, P., Ryu, Y.-H., Skowron, J., et al. 2018, AJ, 155, 121

Paczyński, B. 1986, ApJ, 304, 1

Poleski, R., Skowron, J., Udalski, A., et al. 2014, ApJ, 795, 42

Sahu, K. C. & Sahu, M. S. 1998, ApJ, 508, L147

Shvartzvald, Y., Maoz, D., Udalski, A., et al. 2016, MNRAS, 457, 4089

Shvartzvald, Y., Udalski, A., Gould, A., et al. 2015, ApJ, 814, 111

Shvartzvald, Y., Yee, J. C., Calchi Novati, S., et al. 2017, ApJ, 840, L3

Suzuki, D., Bennett, D. P., Sumi, T., et al. 2016, ApJ, 833, 145

Udalski, A., Ryu, Y.-H., Sajadian, S., et al. 2018, Acta Astron., 68, 1

Wang, J. & Fischer, D. A. 2015, AJ, 149, 14

Wyrzykowski, Ł., Skowron, J., Kozłowski, S., et al. 2011, MNRAS, 416, 2949

Yee, J. C., Shvartzvald, Y., Gal-Yam, A., et al. 2012, ApJ, 755, 102